

SUPERCRITICAL-PHASE THERMAL DECOMPOSITION OF JET FUEL COMPONENTS: MODEL COMPOUND STUDIES

Jian Yu and Semih Eser
Fuel Science Program
Department of Materials Science and Engineering
209 Academic Projects Building
The Pennsylvania State University
University Park, PA 16802

INTRODUCTION

In an advanced aircraft, the fuel is the primary sink for the heat generated on board. With the development of high-speed aircraft, it is expected that the future fuel system will be operating at high-temperature supercritical conditions because of the increased thermal load (Edwards and Zabarnick, 1993). At high-temperature supercritical conditions, the fuel may decompose to form solid deposits. Solid deposition in various fuel system components, such as valves, filters, and fuel lines, could create serious problems in the operation and maintenance of aircraft. It is important to study supercritical fuel decomposition process in order to develop thermally stable jet fuels.

In this work, the thermal decomposition of n-decane ($n\text{-C}_{10}$), n-dodecane ($n\text{-C}_{12}$), n-tetradecane ($n\text{-C}_{14}$), n-butylbenzene (BBZ), n-butylcyclohexane (BCH), decalin (DHN), and tetralin (THN) was studied under supercritical conditions. The results from thermal decomposition of $\text{C}_{10}\text{-C}_{14}$ normal alkanes have been reported previously (Yu and Eser, 1997a, 1997b) and were presented here for completeness. These model compounds were selected because they are typical components found in jet fuels. It has been shown that both petroleum-derived and coal-derived fuels contain significant amounts of long-chain alkanes, alkylbenzenes, and alkylcycloalkanes (Lai and Song, 1995a, 1995b). The coal-derived fuels also contain significant amounts of decalins and tetralins.

EXPERIMENTAL

Most of the model compounds used in this study were obtained from Aldrich. The n-butylbenzene and n-butylcyclohexane were obtained from TCI America. The purities of all compounds were higher than 99%. Decalin consisted of 47.90% of cis-decalin and 51.88% of trans-decalin as well as a small amount of tetralin and other impurities. All model compounds were used as received. Table I shows the critical properties of the model compounds.

Thermal reaction experiments were carried out at 400–475 °C and 10–100 atm (initial pressure) in a Pyrex glass tube reactor and, in some cases, in a 316 stainless steel tubing bomb reactor. A fluidized sand bath was used to heat the reactor. Before an experiment was started, the sand bath was preheated to the desired temperature. The reactor was then plunged into the bath. The heat-up period for the glass tube to reach 450 °C was less than two minutes and the corresponding value for the tubing bomb was about four to five minutes. It was found that the temperature of the sand bath was very uniform and was always within ± 1 °C of the desired temperature after the heat-up period. After a given reaction time the reactor was removed from the bath and was cooled down using pressurized air (the glass tube) or quenched in cool water (the tubing bomb). The reaction products from the tubing bomb experiments were separated into gases and liquids for analysis. The gaseous products from glass tube experiments were not collected because of the extremely low gas yields.

The liquid products were analyzed quantitatively by a Perkin Elmer 8500 GC equipped with a DB-17 capillary column and a flame ionization detector (FID). The compounds in the liquid products were identified by gas chromatography-mass spectrometry (GC-MS) using a Hewlett Packard (HP) 5890 II GC connected with an HP 5971A mass selective detector. The identifications of the major compounds were also made by running standard mixtures. The gaseous products from the tubing bomb experiments were analyzed quantitatively using a Perkin Elmer AutoSystem gas chromatograph (GC) equipped with two different columns and detectors. One stainless steel column packed with 80/100 Chemipack C18 was used to determine the yields of $\text{C}_1\text{-C}_6$ gases with an FID. The other stainless steel column packed with 60/80 Carboxen-1000 was used to determine the yields of H_2 , CO , CO_2 , CH_4 , C_2H_2 , C_2H_4 , and C_2H_6 with a thermal conductivity detector (TCD). The gaseous products were identified and quantified by using standard gas mixtures.

RESULTS AND DISCUSSION

Kinetics. Previous studies show that thermal decomposition of hydrocarbons usually follows a first-order rate law (Steacie, 1946; Fabuss et al., 1964). Therefore, the rate constants were determined by the following first-order expression:

$$k = \frac{1}{t} \ln \frac{1}{1-x} \quad (1)$$

where x is the fraction of the reactant converted (conversion), k is the rate constant (h^{-1}), and t is the reaction time (h). The conversions were obtained from the thermal decomposition experiments in the glass tube reactor at different temperatures for different times. A fixed loading ratio, defined as the ratio of the initial sample volume to the reactor volume, of 0.36 was used in the experiments.

Figure 1 shows the relationship between $\ln[1/(1-x)]$ and time for the thermal decomposition of *n*-butylbenzene. Similar linear relationships between $\ln[1/(1-x)]$ and time were obtained for the decomposition of other model compounds. From the slopes of the lines in Figure 1, the first-order rate constants at different temperatures can be obtained. Table 2 shows the calculated first-order rate constants for the thermal decomposition of seven model compounds. From Table 2 one can see that for the three *n*-alkanes, the first-order rate constant increases with the increasing carbon number (at the same temperature). Among C_{10} hydrocarbons, the rate constant decreases in the order of $\text{BBZ} > \text{n-C}_{10} > \text{BCH} > \text{DHN} > \text{THN}$.

According to the first-order rate constants shown in Table 2, the apparent activation energies (E_a , kcal/mol) and preexponential factors (A , h^{-1}) can be determined using the following Arrhenius law:

$$k = A \exp(-E_a / RT) \quad (2)$$

Figure 2 shows the Arrhenius plots from the thermal decomposition of model compounds. The apparent activation energies and preexponential factors obtained from the Arrhenius plots are also shown in Table 2. The slight differences between the apparent activation energies for the three *n*-alkanes may arise from the experimental uncertainty.

Product Distributions. The reaction products from the thermal decomposition of C_{10} – C_{14} *n*-alkanes under supercritical conditions can be divided into two categories: those from the primary reactions and those from the secondary reactions of the primary products. The primary products include *n*-alkanes from C_1 to C_{m-2} (m = number of carbon atoms in the reactant) and 1-alkenes from C_2 to C_{m-1} . The secondary products include *cis*- and *trans*-2-alkenes, *n*- C_{m-1} , *n*- C_{m+1} , and C_{m-2} to C_{2m-2} normal and branched alkanes. There are also small amounts of cyclopentanes and cyclohexanes. The yields of branched alkanes lighter than the reactant are not significant until high conversions are reached.

The liquid products from thermal decomposition of *n*-butylbenzene can also be divided into the primary products and the secondary products. The primary products include toluene, styrene, ethylbenzene, benzene, allylbenzene, and tetralin. The secondary products include *n*-pentane, 2-methylbutane, *n*-propylbenzene, isopropylbenzene, *sec*-butylbenzene, isobutylbenzene, *n*-pentylbenzene, 1-propylbutylbenzene, 1,3-diphenylpropane, 1,4-diphenylbutane, 1,3-diphenylhexane, and three other C_6 -diphenyls. At higher conversions (> 30%), more than 150 liquid compounds were found. The gaseous products from thermal decomposition of *n*-butylbenzene include hydrogen, methane, ethane, ethylene, propane, and propylene.

The liquid products from *n*-butylcyclohexane thermal decomposition include the primary products cyclohexane, methylenecyclohexane, cyclohexene, methylcyclohexane, vinylcyclohexane, allylcyclohexane, ethylcyclohexane, some C_{10} alkenes and butylcyclohexenes, and the secondary products 1-methylcyclohexene, 3-methylcyclohexene, methylcyclopentane, 1-ethylcyclohexene, and *n*-propylcyclohexane. Some high-molecular-weight compounds, including *n*-pentylcyclohexane, *n*-hexylcyclohexane, several C_7 and C_8 -cyclohexanes, dicyclohexylmethane, dicyclohexylethane, C_7 -dicyclohexyl, and C_8 -dicyclohexyl, were also found. At the highest conversion obtained in this study (39%, 475 °C, 20 min), about 130 peaks were observed from the chromatogram of the liquid products. The gaseous products from thermal decomposition of *n*-butylcyclohexane include hydrogen, methane, ethane, ethylene, propane, propylene, butane, and butene.

The major liquid products from the thermal decomposition of decalin include spiro[4,5]decane, 1-methylcyclohexene, 1-butylcyclohexene, and 1-methylperhydroindan. Also appearing, but in slightly lower yields, are toluene, some C₄-cyclohexenes, n-butylbenzene, and three unidentified compounds which eluted between trans-decalin and tetralin from the GC column. Some minor products include cyclohexane, cyclohexene, methylcyclopentane, methylcyclohexane, 3-methylcyclohexene, methylenecyclohexane, benzene, ethylbenzene, n-butylcyclohexane, tetralin, naphthalene, and some high molecular weight compounds. At 450 °C for 60 min, about 80 compounds were found in the liquid products. The gaseous products include hydrogen, methane, ethane, ethylene, propane, propylene, butane, and butene.

The most abundant liquid product from thermal decomposition of tetralin under supercritical conditions is 1-methylindan, followed by naphthalene, n-butylbenzene, and 2-methylindan. Also appearing, but in lower yields, are n-propylbenzene, ethylbenzene, and toluene. Hydrogen is dominant gaseous product. Other gases include methane, ethane, ethylene, propane, propylene, butane, and butene.

Effects of Supercritical Conditions on Product Distributions. Figure 3 shows the changes in overall molar yields of C₆-C₁₃ n-alkanes, C₆-C₁₃ 1-alkenes, C₆-C₁₂ 2-alkenes, and C₁₄ normal and branched alkanes with the initial reduced pressure from the thermal decomposition of n-C₁₄ at 425 °C for 15 min. The initial reduced pressure ($P_r = P/P_c$) was calculated at the given temperature and loading ratio using the Soave-Redlich-Kwong equation of state (Soave, 1972). It can be seen that the overall yield of C₆-C₁₃ n-alkanes increases and that of C₆-C₁₃ 1-alkenes decreases as pressure increases. The large changes in product distributions with pressure occur in the near-critical region. While the overall yields of C₆-C₁₂ 2-alkenes and C₁₄ alkanes are low at low-pressure sub-critical conditions, their yields become significant at high-pressure supercritical conditions.

Figure 4 shows the effects of pressure on product distributions from the thermal decomposition of n-butylbenzene at 425 °C for 15 min. The major primary products are toluene and styrene. It can be seen that as pressure increases, the styrene yield decreases and the toluene yield increases. In contrast to a higher yield of styrene in the sub-critical region, a higher toluene yield is obtained in the far supercritical region. It is clear that high-pressure supercritical conditions suppress the formation of styrene. On the other hand, the yields of the high-molecular-weight products increase with the increasing pressure. Although not shown in Figure 4 because of low yields, the yields of some other high-molecular-weight products, such as 1-propylbutylbenzene and three other C₆-diphenyls, also increase with the increasing pressure.

CONCLUSIONS

Supercritical-phase thermal decomposition of jet fuel model compounds follows a first-order kinetics. Among the compounds studied, n-butylbenzene exhibited the highest reactivity, followed by n-C₁₄, n-C₁₂, n-C₁₀, n-butylcyclohexane, decalin, and tetralin.

Thermal decomposition of C₁₀-C₁₄ n-alkanes under supercritical conditions gave high yields of C₃ n-alkanes and significant amounts of heavy alkanes which are usually not observed under low-pressure sub-critical conditions. The pyrolyses of n-butylbenzene and n-butylcyclohexane were dominated by side-chain cracking. The formation of significant amounts of diphenylalkanes from pyrolysis of n-butylbenzene under supercritical conditions indicates that the reaction mechanism under these conditions is different from that under lower-pressure sub-critical conditions. The thermal decomposition of decalin and tetralin under high-pressure supercritical conditions was dominated by isomerization reactions. This is different from the results obtained under low-pressure and high-temperature conditions where cracking reactions (for decalin) or dehydrogenation reactions (for tetralin) dominate.

ACKNOWLEDGMENT

This work was supported by the U.S. Department of Energy, Pittsburgh Energy Technology Center, and the Air Force Wright Laboratory/Aero Propulsion and Power Directorate, Wright-Patterson AFB. Funding was provided by the U.S. DOE under Contract DE-FG22-92PC92104. We would like to express our gratitude to Prof. Harold H. Schobert of Penn State for his support. We thank Mr. W. E. Harrison III and Dr. T. Edwards of AFWL/APPD and Dr. S. Rogers of PETC for many helpful discussions.

REFERENCES

1. Daubert, T. E.; Danner, R. P. *Physical and Thermodynamic Properties of Pure Chemicals; Design Institute for Physical Property Data, AIChE: Washington, DC, 1992.*
2. Edwards, T.; Zabarnick, S. *Ind. Eng. Chem. Res.* **1993**, *32*, 3117.
3. Fabuss, B. M.; Smith, J. O.; Satterfield, C. N. *Adv. Petro. Chem. Refin.* **1964**, *9*, 157-201.
4. Lai, W.-C.; Song, C. *Fuel*, **1995a**, *74*, 1436.
5. Lai, W.-C.; Song, C. In *Advanced Thermally Stable Jet Fuels*, Technical Progress Report, April 1995 – June 1995, The Pennsylvania State University, August 1995b.
6. Soave, G. *Chem. Eng. Sci.* **1972**, *27*, 1197.
7. Steacie, E. W. R. *Atomic and Free Radical Reactions*; Reinhold: New York, 1946.
8. Teja, A. S.; Lee, R. J.; Rosenthal, D. J.; Anselme, M. *Fluid Phase Equil.* **1990**, *56*, 153.
9. Yu, J.; Eser, S. *Ind. Eng. Chem. Res.* **1997a**, *36*, 574.
10. Yu, J.; Eser, S. *Ind. Eng. Chem. Res.* **1997b**, *36*, 585.

Table 1. Critical Properties of Model Compounds

	T_c , °F	T_c , °C	P_c , psia	P_c , atm
n-C ₁₀ ^a	652	345	304	20.7
n-C ₁₂ ^a	725	385	262	17.9
n-C ₁₄ ^a	786	419	228	15.5
n-butylbenzene ^b	729	387	419	28.5
n-butylcyclohexane ^b	741	394	373	25.4
cis-decalin ^b	804	429	470	32.0
trans-decalin ^b	777	414	411	28.0
tetralin ^b	837	447	525	35.7

^a Teja et al. (1990). ^b Daubert and Danner (1992).

Table 2. Kinetic Parameters for Thermal Decomposition of Model Compounds

reactant	rate constant, h ⁻¹				E_a^a	log A ^b
	400 °C	425 °C	450 °C	475 °C		
n-C ₁₀	0.0341	0.174	0.758		60	18.0
n-C ₁₂	0.0453	0.231	1.13		62	18.8
n-C ₁₄	0.0640	0.364	1.67		63	19.3
BBZ	0.0891	0.422	1.72		57	17.6
BCH		0.0613	0.313	1.40	65	19.1
DHN		0.0238	0.132	0.669	69	20.1
THN		0.0090	0.0370	0.139	58	16.1

^a E_a , apparent activation energy in kcal/mol. ^b A, preexponential factor in h⁻¹.

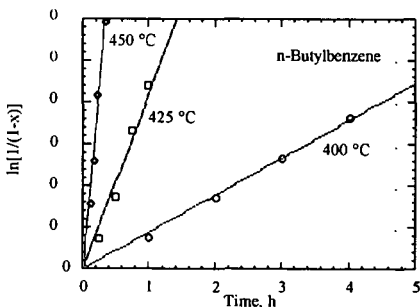


Figure 1. $\ln[1/(1-x)]$ versus time from thermal decomposition of n-butylbenzene.

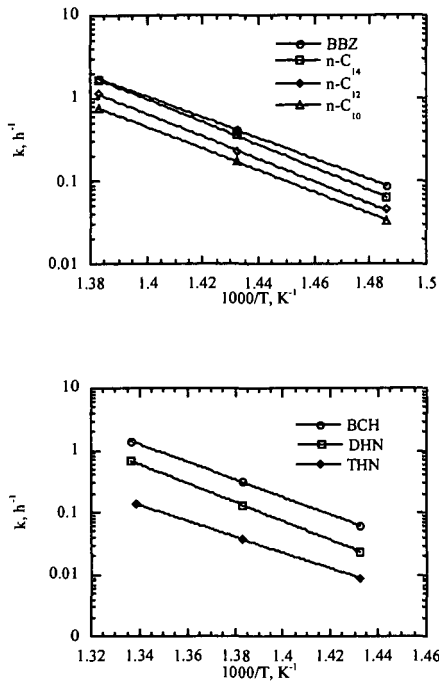


Figure 2. Arrhenius plots from thermal decomposition of jet fuel model compounds

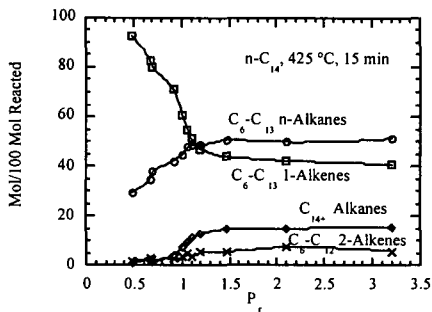


Figure 3. Product yields versus P_r from $n\text{-C}_{14}$ at $425\text{ }^\circ\text{C}$ for 15 min.

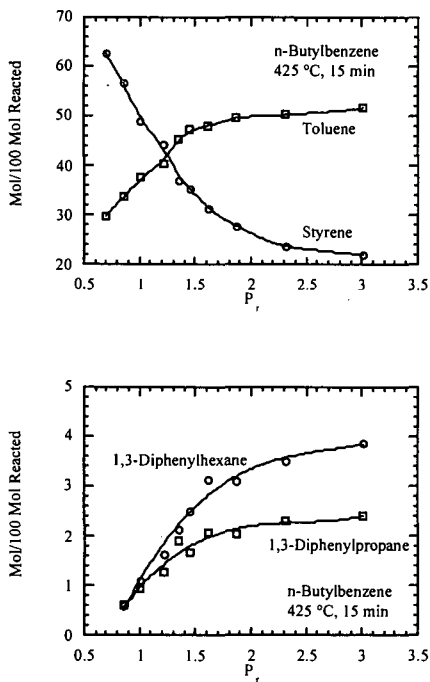


Figure 4. Product yields versus P_r from $n\text{-butylbenzene}$ at $425\text{ }^\circ\text{C}$ for 15 min.